An Intramolecular N–H···(μ-H)Re_2 Dihydrogen Bond and a Novel μ_3-η^2 Coordination Mode of the Pyrazolate Anion on a Triangular Cluster Face

Tiziana Beringhelli,*[a] Giuseppe D'Alfonso,[a] Monica Panigati,[a] Pierluigi Mercandelli,*[b] and Angelo Sironi[b]

Abstract: The quantitative addition of pyrazole (Hpz) to the 44 valence-electron, triangular cluster anion $[Re_3(\mu_3\text{-H})(\mu\text{-H})_3(CO)_9]^-$ gives the novel unsaturated anion $[Re_3(\mu\text{-H})_4(CO)_9(Hpz)]^-$ (**1**, 46 valence electrons), which contains a pyrazole molecule that is terminally coordinated on a cluster vertex. Solid-state X-ray and IR analyses reveal a rather weak hydrogen-bonding interaction between the NH proton and one of the hydrides bridging the opposite triangular cluster edge ($\Delta H^\circ = -3.1$ kcal mol^{-1} from the Iogansen equation). Both IR and NMR data indicate that such a proton–hydride interaction is maintained in the major conformer present in CD_2Cl_2, but also provide evidence of the presence of minor conformers of **1** in which the NH proton is involved in an *inter*molecular hydrogen bond with the solvent. The μ-H···HN bond length evaluated in solution through the T_1 minimum value (2.07 Å) and that determined in the solid state by X-ray diffraction (2.05 Å) are in good agreement. NMR experiments show that, in acetone, *inter*molecular N–H···solvent interactions replace the *intra*molecular dihydrogen bond. At room temperature in CH_2Cl_2, the pyrazole ligand in **1** is labile and **1** slowly "disproportionates" to $[Re_3(\mu_3\text{-H})(\mu\text{-H})_3(CO)_9]^-$ and $[Re_3(\mu\text{-H})_3(CO)_9(\mu\text{-}\eta^2\text{-pz})(Hpz)]^-$, with H_2 evolution. Slow H_2 evolution also leads to the formation of the anion $[Re_3(\mu\text{-H})_3(CO)_9(pz)]^-$ (**5**), in which the pyrazolate anion adopts a novel μ_3-η^2-coordination mode, as revealed by a single-crystal X-ray analysis. The analysis of the bond lengths indicates that the pyrazolate anion in **5** acts as a six-electron donor, with loss of the aromaticity. The formation of **5** from **1** is much faster in solvents with a high dielectric constant, such as acetone or DMF. Anion **5** was also obtained from the reaction of pyrazole with $[Re_3(\mu\text{-H})_3(CO)_9(\mu_3\text{-}CH_3)]^-$ through the intermediate formation of two isomeric addition derivatives and following CH_4 evolution.

Keywords: cluster compounds · hydride ligands · hydrogen bonds · NMR spectroscopy · pyrazole · structure elucidation

Introduction

The relevance of hydrogen bonding in many fields of chemistry, particularly in supramolecular chemistry and in biochemistry, is well known.[1] In the past ten years, several new types of hydrogen bonding have been identified that involve transition metals or their complexes, such as the X–H···M, M–H···X or M–H···H–X interactions (X most often being N, O, or S).[2] Particular attention has been devoted to the last type of interaction,[3] in which a σ M–H bond acts as the electron donor (or the hydrogen bond acceptor). These interactions, for which the term "dihydrogen bond" has been coined,[4] were found to be fairly strong (up to 7.0 kcal mol^{-1}, with H···H bond lengths as low as 1.7 Å), sometimes competing favourably with conventional hydrogen bonds. The first examples of these interactions involved proton donors belonging to ligands bound to the same metal centre that also carried the hydrido ligand.[5] Subsequently, a number of intermolecular H···H proton–hydride interactions have been evidenced,[3, 6] and it has been suggested that they play an important role as intermediates in the protonation pathway to form dihydrogen complexes.[7]

A particular type of intramolecular dihydrogen bond is that occurring in transition metal clusters, in which the hydrogen bond donor and acceptor moieties are bound to different metal atoms, but are in a definite mutual relationship, being confined by the cluster skeleton. A few examples of such interactions have been reported so far,[8] and it has been shown that they are able to direct the stereochemistry of the

[a] Prof. T. Beringhelli, Prof. G. D'Alfonso, Dr. M. Panigati
Dipartimento di Chimica Inorganica, Metallorganica e Analitica
Università di Milano, via Venezian 21
20133 Milano (Italy)
Fax: (+39) 02-50314405
E-mail: tiber@csmtbo.mi.cnr.it

[b] Dr. P. Mercandelli, Prof. A. Sironi
Dipartimento di Chimica Strutturale e Stereochimica Inorganica
Università di Milano, via Venezian 21
20133 Milano (Italy)
Fax: (+39) 02-50314454
E-mail: pierluigi.mercandelli@unimi.it

  0947-6539/02/0823-5340 $ 20.00+.50/0

reactions, to dictate the conformation of the ligand and to influence its dynamics and reactivity.

Previously, we reported the spectroscopic and diffractometric characterisation of the trirhenium carbonyl cluster anion $[Re_3(\mu\text{-}H)_3(CO)_9(\mu\text{-}\eta^2\text{-}pz)(Hpz)]^-$, in which we observed that the preferred conformation of the terminal pyrazole ligand arose from a hydrogen bond between the NH proton of the pyrazole ligand and the aromatic π-electrons of the pyrazolato ligand bridging on the opposite edge of the same cluster.[9] We report here on a new solid-state and solution study concerning a trirhenium cluster containing a terminally coordinated pyrazole, namely the anion $[Re_3(\mu\text{-}H)_4(CO)_9(Hpz)]^-$ (**1**). The X-ray and NMR data have shown that in this species the preferred conformation of the pyrazole ligand, both in the solid state and in solution, is also attributable to an intramolecular hydrogen bond, which in this case involves a nonclassical H···H interaction between the NH proton of pyrazole and one of the two hydrides bridging the basal edge of the triangular cluster anion. This proton–hydride interaction slowly gives rise to H_2 evolution, to produce the $[Re_3(\mu\text{-}H)_3(CO)_9(pz)]^-$ anion, stabilised by the novel coordination mode of the pyrazolate anion, $\mu_3\text{-}\eta^2$, that bridges the three cluster vertices.

Results and Discussion

The addition of a slight excess of pyrazole to a solution of the "super-unsaturated" triangular cluster anion $[Re_3(\mu_3\text{-}H)(\mu\text{-}H)_3(CO)_9]^-$ (**2**, 44 valence electrons)[10] in CH_2Cl_2 at room temperature gives a quantitative yield of the novel unsaturated anion $[Re_3(\mu\text{-}H)_4(CO)_9(Hpz)]^-$ [**1**, 46 valence electrons, Eq. (1)], containing a pyrazole molecule terminally coordinated on a cluster vertex (Scheme 1).

$$[Re_3(\mu_3\text{-}H)(\mu\text{-}H)_3(CO)_9]^- + Hpz \rightarrow [Re_3(\mu\text{-}H)_4(CO)_9(Hpz)]^- \quad (1)$$

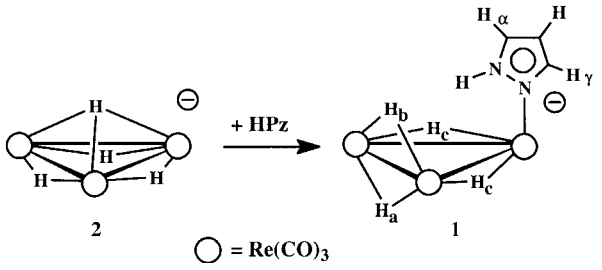

Scheme 1.

The ^1H NMR spectrum (CD_2Cl_2, 298 K) shows only one set of hydridic signals (three resonances at $\delta = -7.73$, -9.03 and -9.68, ratio 1:1:2), attributable to the axial derivative shown in Scheme 1. The solid-state conformation of pyrazole has been revealed by a single-crystal X-ray diffractometric analysis (and confirmed by IR data), while the solution conformation in different solvents has been investigated by IR and NMR spectroscopy.

Solid-state characterisation of the anion $[Re_3(\mu\text{-}H)_4(CO)_9(Hpz)]^-$ (1):

*X-ray crystal structure of [PPh$_4$]**1***: The molecular structure of anion **1**, as determined in a crystal of its $[PPh_4]^+$ salt, is depicted in Figure 1 (with a partial labelling scheme). A selection of bond parameters is reported in Table 1.

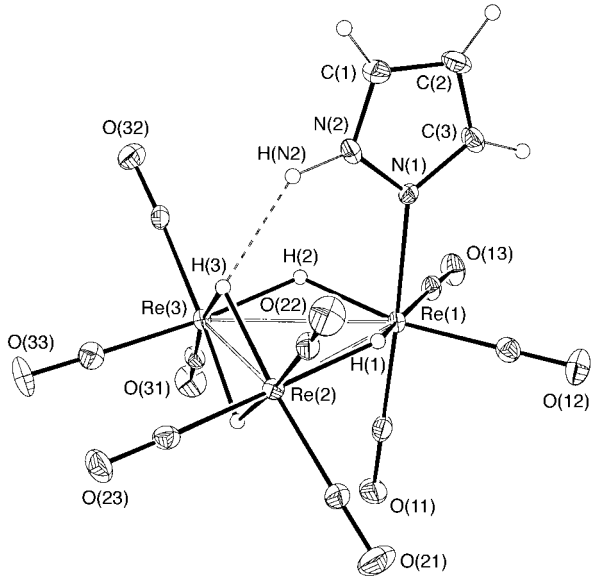

Figure 1. ORTEP drawing of the $[Re_3(\mu\text{-}H)_4(CO)_9(Hpz)]^-$ anion (**1**) with a partial labelling scheme. Thermal ellipsoids are drawn at the 30% probability level. Hydrogen atoms were given arbitrary radii.

Anion **1** possesses an overall idealised C_s symmetry and contains a metal core of three Re atoms arranged as an isosceles triangle, nine terminal carbonyls, three to each rhenium atom, a pyrazole moiety and four edge-bridging hydrido ligands. With reference to the related cluster $[Re_3(\mu\text{-}H)_4(CO)_{10})]^-$,[11] one axial carbonyl of the $[Re(CO)_4]$ vertex is actually replaced by a monodentate *N*-coordinated pyrazole. With regard to the bonding interactions around the rhenium atoms, if the direct metal–metal interactions are neglected, each metal attains a distorted octahedral coordination.

Cluster **1** shows two long Re–Re distances (mean value 3.196 Å) and one shorter interaction (2.820 Å) in correspondence with the $Re(\mu\text{-}H)_2Re$ formal double bond; a similar pattern has been observed in the related unsaturated clusters $[Re_3(\mu\text{-}H)_4(CO)_9L]^-$ (L = carbonyl, pyridine, or triphenylphosphine).[11, 12]

As shown in Figure 1, the HN(2) proton of the pyrazole ligand bound to Re(1) forms a hydrogen bond with the hydride H(3), bridging the opposite cluster edge Re(2)–Re(3). Dihydrogen bonds involving bridging hydrides are uncommon; a search in the Cambridge Structural Database[13] for crystal structures exhibiting (N,O,S)–H···(μ-H) contacts shorter than the sum of van der Waals radii (2.34 Å) led to three matches only,[14] in which the $d(H\cdots H)$ ranges from 1.72 to 2.06 Å.[15] In anion **1**, the distance between HN(2) and H(3) is 2.047 Å; this distance has been computed with idealised positions[16] for both the hydrogen atoms, even if they were clearly evidenced in a difference Fourier map, in

  0947-6539/02/0823-5341 $ 20.00+.50/0

Table 1. Selected bond lengths [Å] and angles [°] for the trinuclear complexes **1** and **5**.

	1	**5**		**1**	**5**
Re(1)–Re(2)	3.1969(16)	3.1801(12)	Re(2)–C(22)	1.907(6)	1.908(15)
Re(1)–Re(3)	3.1961(16)	3.1631(12)	Re(2)–C(23)	1.926(6)	1.933(12)
Re(2)–Re(3)	2.8198(12)	2.9536(11)	Re(3)–C(31)	1.916(6)	1.865(13)
Re(1)–N(1)	2.201(4)	2.171(8)	Re(3)–C(32)	1.911(6)	1.929(13)
Re(2)–N(2)		2.236(7)	Re(3)–C(33)	1.925(6)	1.889(11)
Re(3)–N(2)		2.252(8)	N(1)–N(2)	1.336(5)	1.367(11)
Re(1)–C(11)	1.910(6)	1.913(12)	N(1)–C(3)	1.349(6)	1.310(12)
Re(1)–C(12)	1.912(6)	1.880(12)	N(2)–C(1)	1.325(6)	1.354(12)
Re(1)–C(13)	1.918(6)	1.868(11)	C(1)–C(2)	1.361(7)	1.329(18)
Re(2)–C(21)	1.925(6)	1.897(12)	C(2)–C(3)	1.387(7)	1.398(19)
Re(2)-Re(1)-Re(3)	52.346(11)	55.502(11)	C(21)-Re(2)-C(23)	92.5(2)	89.7(5)
Re(1)-Re(2)-Re(3)	63.81(4)	61.957(13)	C(22)-Re(2)-C(23)	89.6(2)	91.6(6)
Re(1)-Re(3)-Re(2)	63.84(4)	62.541(13)	Re(1)-Re(3)-N(2)		63.1(2)
Re(2)-Re(1)-N(1)	94.50(10)	64.2(2)	Re(1)-Re(3)-C(31)	96.64(15)	109.6(4)
Re(2)-Re(1)-C(11)	83.57(15)	108.8(3)	Re(1)-Re(3)-C(32)	112.83(15)	95.9(4)
Re(2)-Re(1)-C(12)	107.28(15)	104.0(4)	Re(1)-Re(3)-C(33)	156.21(16)	158.0(4)
Re(2)-Re(1)-C(13)	161.07(15)	155.4(4)	Re(2)-Re(3)-N(2)		48.60(19)
Re(3)-Re(1)-N(1)	93.89(10)	63.3(2)	Re(2)-Re(3)-C(31)	133.59(15)	127.7(4)
Re(3)-Re(1)-C(11)	83.79(15)	107.6(3)	Re(2)-Re(3)-C(32)	135.69(15)	139.8(3)
Re(3)-Re(1)-C(12)	159.06(15)	156.4(4)	Re(2)-Re(3)-C(33)	94.38(16)	98.8(4)
Re(3)-Re(1)-C(13)	109.41(15)	104.0(4)	N(2)-Re(3)-C(31)		172.5(4)
N(1)-Re(1)-C(11)	177.59(18)	170.4(4)	N(2)-Re(3)-C(32)		91.9(4)
N(1)-Re(1)-C(12)	92.51(18)	98.7(5)	N(2)-Re(3)-C(33)		96.2(4)
N(1)-Re(1)-C(13)	91.64(18)	95.5(4)	C(31)-Re(3)-C(32)	90.3(2)	90.5(5)
C(11)-Re(1)-C(12)	89.5(2)	89.3(5)	C(31)-Re(3)-C(33)	91.9(2)	90.8(5)
C(11)-Re(1)-C(13)	89.7(2)	89.4(5)	C(32)-Re(3)-C(33)	89.2(2)	91.8(5)
C(12)-Re(1)-C(13)	90.3(2)	92.3(5)	Re(1)-N(1)-N(2)	125.8(3)	110.1(5)
Re(1)-Re(2)-N(2)		62.8(2)	Re(1)-N(1)-C(3)	130.2(3)	141.6(9)
Re(1)-Re(2)-C(21)	94.59(16)	108.8(3)	Re(2)-N(2)-Re(3)		82.3(2)
Re(1)-Re(2)-C(22)	110.48(15)	98.0(4)	Re(2)-N(2)-N(1)		108.6(5)
Re(1)-Re(2)-C(23)	158.62(15)	159.1(3)	Re(2)-N(2)-C(1)		129.6(7)
Re(3)-Re(2)-N(2)		49.1(2)	Re(3)-N(2)-N(1)		105.2(5)
Re(3)-Re(2)-C(21)	132.64(16)	126.1(3)	Re(3)-N(2)-C(1)		121.7(7)
Re(3)-Re(2)-C(22)	136.01(16)	142.1(4)	N(2)-N(1)-C(3)	103.9(4)	108.3(9)
Re(3)-Re(2)-C(23)	96.83(16)	99.5(3)	N(1)-N(2)-C(1)	113.2(4)	106.2(8)
N(2)-Re(2)-C(21)		171.3(4)	N(2)-C(1)-C(2)	107.0(5)	111.2(12)
N(2)-Re(2)-C(22)		93.7(4)	C(1)-C(2)-C(3)	105.3(5)	104.5(10)
N(2)-Re(2)-C(23)		98.1(4)	N(1)-C(3)-C(2)	110.7(5)	109.9(12)
C(21)-Re(2)-C(22)	90.2(2)	89.7(5)			

order to avoid the systematic errors associated with hydrogen atom positions determined by X-ray diffraction.

The presence of this dihydrogen-bonding interaction is confirmed by the sterically unfavourable conformation assumed by the pyrazole ligand, which, lying in the idealised mirror plane of the molecule, strongly interacts with the diagonal carbonyl ligands bound to the Re(μ-H)$_2$Re moiety. This interaction results in a significant tilting of the coordination octahedra at the rhenium atoms, as evidenced by the large mean value of the Re(1)-Re(2,3)-C(22,32) angles (111.7°, to be compared to 103.8° in the parent compound $[Re_3(\mu\text{-}H)_4(CO)_{10}]^-$). Indeed, in the closely related complex $[Re_3(\mu\text{-}H)_4(CO)_9(py)]^-$,[12] in which a N–H···H dihydrogen bond cannot occur, the pyridine ligand lies perpendicular to the idealised mirror plane of the molecule, assuming a conformation that minimises the interaction with the [(CO)$_3$Re(μ-H)$_2$Re(CO)$_3$] moiety. An analogous sterically unfavourable conformation of a pyrazole ligand has been reported for the anion $[Re_3(\mu\text{-}H)_3(CO)_9(\mu\text{-}\eta^2\text{-}pz)Hpz]^-$,[9] in which the pyrazole NH hydrogen atom is likewise involved in a hydrogen-bonding interaction with the π electrons of the pyrazolato ligand bridging the opposite edge of the cluster.

Crystalline [PPh$_4$]**1** presents additional interesting structural features. A short *inter*molecular N–H···O hydrogen-bonding interaction is observed between the hydrogen atom of the pyrazole ligand and one carbonyl ligand of a symmetry-related anion, resulting in the formation of a dimer linked by two bifurcated hydrogen bonds (Figure 2). The structural parameters of this interaction are listed in Table 2.

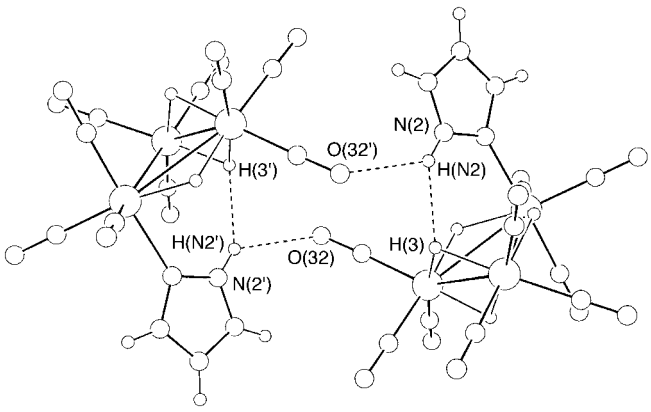

Figure 2. Hydrogen-bonding interactions in the crystal structure of [NEt$_4$][Re$_3$(μ-H)$_4$(CO)$_9$(Hpz)].

0947-6539/02/0823-5342 $ 20.00+.50/0 *Chem. Eur. J.* **2002**, *8*, No. 23

Table 2. Relevant hydrogen bond parameters (bond lengths [Å] and angles [°]) for $[PPh_4]$**1**.[a]

N(2)–H(N2)	1.024
H(N2)···H(3)	2.047
H(N2)···O(32′)	2.291
N(2)···H(3)	2.937
N(2)···O(32′)	3.046(6)
N(2)–H(N2)···H(3)	143.8
N(2)–H(N2)···O(32′)	129.5
H(3)–H(N2)···O(32′)	86.6

[a] Primes refer to symmetry-related atoms $(-x, -y, 2-z)$.

Infrared evidence of the dihydrogen bond: The solid-state IR spectrum shows that the ν(NH) band of $[NEt_4]$**1** (3288 cm^{-1}, $\Delta\nu_{1/2} = 41\ cm^{-1}$) is broader and shifted to a lower frequency with respect to that of a bona fide model compound that contains a pyrazole molecule coordinated to a rhenium cluster and not involved in hydrogen-bonding interactions (3436 cm^{-1}, $\Delta\nu_{1/2} = 21\ cm^{-1}$).[17] As a model compound, we have synthesised the new complex $[Re_3(\mu\text{-}H)_3(CO)_{11}(Hpz)]$ (**3**) (see the Experimental Section): this species contains a pyrazole molecule terminally coordinated to a vertex of a triangular rhenium cluster, but, with respect to **2**, the three hydrides lie far away from the NH proton of the ligand and therefore no N–H···hydride interaction can be present in **3**.

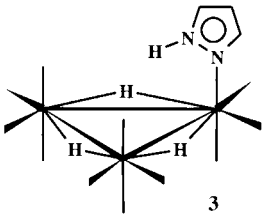

3

The hydrogen bond strength can be estimated from IR data through an empirical equation proposed by Iogansen [Eq. (2)],[18] which correlates the enthalpy of the hydrogen bond with the change in position of the proton-donor stretching band ($\Delta\nu = \nu(NH)_{free} - \nu(NH)_{bonded}$) upon hydrogen-bond formation.

$$-\Delta H^\circ = \frac{18\,\Delta\nu}{\Delta\nu + 720} \qquad (2)$$

In the present case, $\Delta\nu = 148\ cm^{-1}$ (if **3** is used as the "hydrogen-bond free" reference compound), and therefore $\Delta H^\circ = -3.1\ kcal\,mol^{-1}$. Such a value, being at the lower end of the range of values found for a nonclassical X–H···H–Y hydrogen bond (3–7 $kcal\,mol^{-1}$),[2, 3] indicates a rather weak interaction. Therefore, we have also investigated the possible persistence of such an interaction in solution.

Solution characterisation of the anion $[Re_3(\mu\text{-}H)_4(CO)_9(Hpz)]^-$ (1):

Infrared evidence: At room temperature, in dilute solutions of **1** in CH_2Cl_2 (≈0.02 M), the ν(NH) band of **1** (3326 cm^{-1}, $\Delta\nu_{1/2} = 58\ cm^{-1}$) is shifted to lower wavenumbers and broadened with respect to pure pyrazole in the same conditions of solvent, temperature and concentration (3459 cm^{-1}, $\Delta\nu_{1/2} = 27\ cm^{-1}$).[19] Moreover, at further variance with the behaviour of free pyrazole, the position and the bandwidth of the ν(NH) band of the anion **1** do not change with the concentration (from 0.012–0.11 M). This data suggests that the intramolecular dihydrogen bond also exists in solution.

In all the samples of **1** examined in CH_2Cl_2 (including isolated crystals, salts of either $[NEt_4]^+$ or $[PPh_4]^+$), a second weaker band is also observed at $\nu = 3421\ cm^{-1}$ (Figure 3c). The position of this additional absorption is almost identical to that of $[Re_3(\mu\text{-}H)_3(CO)_{11}(Hpz)]$ (**3**) in CH_2Cl_2 (Figure 3b).[21] Such a band is therefore attributable to the ν(NH) of different conformers of **1**, in which the NH proton is involved in *inter*molecular hydrogen bonding with the solvent.

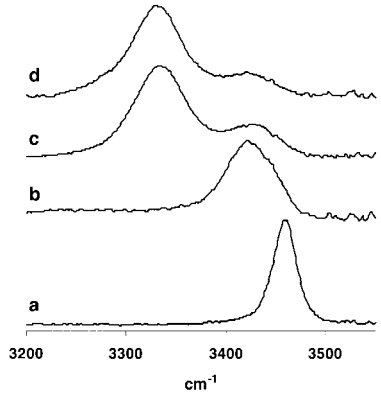

Figure 3. IR spectra in the ν(NH) region in CH_2Cl_2 solution: a) free pyrazole (≈0.02 M); b) the model compound $[Re_3(\mu\text{-}H)_3(CO)_{11}(Hpz)]$ (**3**); c) the anion $[Re_3(\mu\text{-}H)_4(CO)_9(Hpz)]^-$ (**1**), 0.024 M at room temperature; d) the anion **1** at 223 K.

Variable-temperature measurements showed that the ratio between the integrals of the two bands varied with the temperature, on passing from ≈4 at room temperature to ≈9 at 223 K. This ratio can be viewed as the constant of the equilibrium from minor conformers to the major one, and a van't Hoff plot provided the thermodynamic data of such an equilibrium: $\Delta H^\circ = -1.3(1)\ kcal\,mol^{-1}$, $\Delta S^\circ = -1.6(1)\ cal\,mol^{-1}\,K^{-1}$. Assuming any other factors affecting the stability of the different conformers to be negligible, this ΔH° value would provide the enthalpy difference between the intramolecular nonclassical N–H···H–Re interaction and the intermolecular classical N–H···Cl–C hydrogen bond.

NMR studies: NMR solution experiments have provided further evidence of the presence of dihydrogen bonding within the cluster. At 298 K in CD_2Cl_2, the chemical shift of the protonic NH resonance of **1** ($\delta = 10.24$) is similar to those of free pyrazole and of pyrazole coordinated in the reference compound **3** ($\delta = 10.36$ and 10.12, respectively, at the same concentration). However, the temperature dependence of the chemical shifts is quite different in the three species (Table 3), since the δ value of **1** remains substantially unchanged, whilst those of the other two compounds undergo a downfield shift when the temperature is decreased. For free pyrazole the marked decrease is mainly attributable to the formation of oligomers,[20, 22, 23] while the (smaller) shift observed for pyrazole coordinated in **3** is in agreement with the expected increase of *inter*molecular N–H···$ClCH_2Cl$ interactions on lowering the temperature. In contrast, the invariance of the chemical shift in anion **1** is what is expected for a proton involved in an *intra*molecular hydrogen-bonding interaction.

  0947-6539/02/0823-5343 $ 20.00+.50/0

Table 3. Variable-temperature ^{1}H NMR data for the NH resonance of free or bound pyrazole in different complexes (concentration ≈ 0.025 M for all the species).

T[K]	CD_2Cl_2			[D$_6$]acetone	
	Free Hpz	[PPh_4]**1**	**3**	Free Hpz	[NEt_4]**1**
298	10.36	10.24	10.12	12.06	11.86
273	10.52	10.26		12.21	12.08
253	10.85	10.26		12.32	12.26
243			10.34		
213	12.41	10.23	10.57	12.54	12.60
193	13.42	10.21		12.63	12.76

Furthermore, a two-dimensional NOESY experiment at 298 K shows that the NH proton ($\delta = 10.24$) exhibits strong anti-phase cross-peaks not only with the α hydrogen of the pyrazole ligand ($\delta = 7.40$), but also with two of the three hydridic signals (Figure 4). The stronger correlation is observed for the signal of intensity 1 at higher field ($\delta = -9.03$), and this allows its assignment to the H_b hydride bridging the

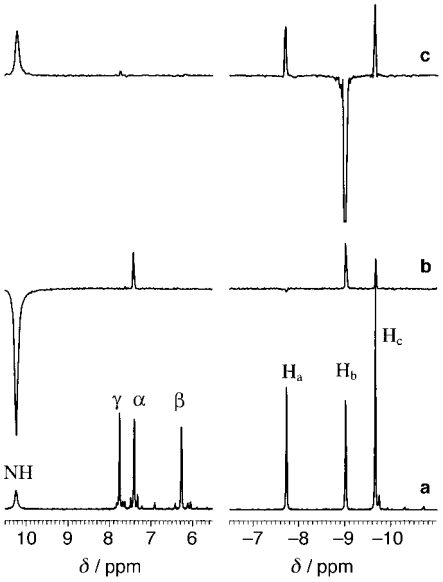

Figure 4. Relevant traces of a ^{1}H two-dimensional NOESY experiment performed on a CD_2Cl_2 solution of anion **1**: a) reference one-dimensional ^{1}H spectrum; b) row corresponding to the NH resonance; c) row corresponding to H_b (4.7 T, 298 K, $\tau_m = 1.0$ s).

base of the triangle in the *syn* position with respect to the pyrazole molecule (Scheme 1). The weaker correlation (volume ratio of the relevant cross-peaks ≈ 3) is observed for the signal assigned to the two H_c hydrides that bridge the cluster edges ($\delta = -9.68$). These results prove that the intramolecular dihydrogen interaction is also maintained in solution at room temperature.

The longitudinal relaxation times, T_1, for the cluster hydrides and the NH proton, measured from 183– 273 K, are reported in Table 4 and plotted as $\ln T_1$ versus $1/T$ in Figure 5. The T_1 measured for the bridging hydride H_b are always shorter than those of all the other hydrogen atoms and, in particular, shorter than those of the H_a hydride, located in the opposite side of the cluster plane, away from the pyrazole. This indicates the presence of an extra contribution to the

Table 4. Temperature dependence of T_1 values[ms] for the hydrides and the NH proton of anion **1** in CD_2Cl_2 (4.7 T).

T[K]	NH	H_a	H_b	H_c
273	930	595	440	585
253	625	402	297	398
223	320	237	168	221
213	274	196	142	180
203	227	162	117	151
193	205	147	108	132
183	210	140	110	126

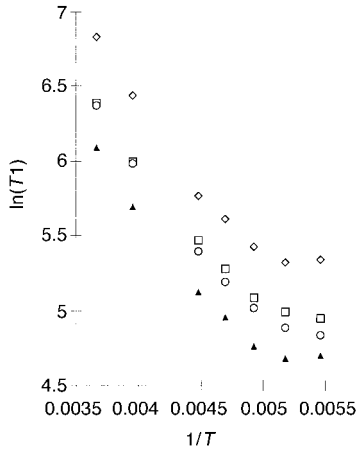

Figure 5. Temperature dependence of the longitudinal relaxation times of the hydridic and NH resonances in anion **1** (4.7 T, CD_2Cl_2): ▲ H_b, ○ H_c, □ H_a, and ◇ NH.

relaxation of H_b, probably the dipolar effect of the close NH hydrogen of pyrazole. The difference between the relaxation rate of H_b and that of H_a gives an estimate of the dipolar contribution of the pyrazole NH to the relaxation of H_b. The occurrence of a minimum in the temperature course of T_1's and, therefore, the knowledge of τ_c[24] allowed the calculation of the distance r_{H-H} between the NH proton and the *syn* hydride. The obtained value, 2.07(8) Å, gives good agreement with that obtained in the solid state by X-ray diffraction (2.05 Å).

Careful inspection of 2D-NOESY experiments performed at 298 K in CD_2Cl_2 with various mixing times (1–3 s), also shows weaker nOe cross-peaks between the γ proton of pyrazole ($\delta = 7.66$) and the H_c hydrides bridging the cluster edges, together with another, even weaker, peak with the *syn* H_b hydride.[25] These correlations suggest that, as observed in IR measurements, under these conditions minor amounts of other conformers exist in which the pyrazole ligand is rotated around the Re–N bond to allow the formation of an intermolecular hydrogen bond between the NH proton and solvent molecules.

*Solvent dependence of the preferred conformation in **1***: The preferred conformation of the pyrazole ligand in solution is solvent dependent. Indeed, in a proton-acceptor solvent such as acetone, all the NMR parameters described above reveal a different balance between inter- and intramolecular interactions.

0947-6539/02/0823-5344 $ 20.00+.50/0 *Chem. Eur. J.* **2002**, *8*, No. 23

A two-dimensional NOESY experiment performed at 300 K (Figure 6) shows that H_b has comparable correlation cross-peaks with the NH or the γ protons of bound pyrazole, indicating that in this solvent comparable amounts of different conformers are present, in some of which the pyrazole

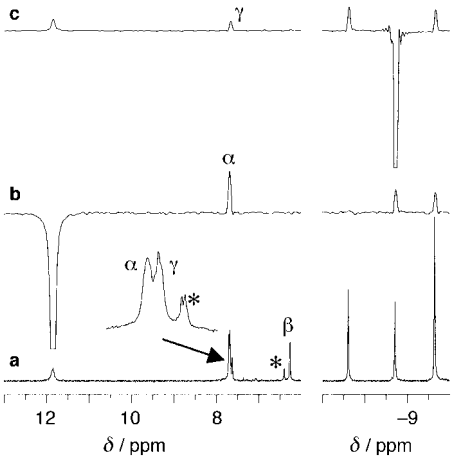

Figure 6. Relevant traces of a ^{1}H two-dimensional NOESY experiment performed on a [D$_6$]acetone solution of anion **1**: a) reference one-dimensional ^{1}H spectrum; b) row corresponding to the NH resonance; c) row corresponding to H_b (7.1 T, 298 K, $\tau_m = 2.0$ s). The asterisks indicate resonances of the anion **5**, which forms rather quickly from **1** in acetone.

molecules engage in hydrogen bonds with the solvent molecules.[26] In agreement with this, the chemical shift of the NH resonance of **1** exhibits a temperature dependence quite similar to that of free pyrazole (Table 3),[27] namely, the downfield shift with decreasing temperature, which is typical of intermolecular hydrogen-bonding interactions with the solvent.[28]

Moreover, at low temperatures, the T_1 values of the three hydrides are almost identical (Table 5) and only small differences are observed on increasing the temperature; this is probably caused by unfavourable entropic contributions to intermolecular interactions.

Table 5. T_1 values [ms] for hydrides and NH proton of anion **1** at different temperatures in [D$_6$]acetone (7.1 T).

T[K]	NH	H_a	H_b	H_c
253	1350	740	648	685
223	655	360	320	330
203	507	253	226	232

Lability of the pyrazole ligand in 1 in solution: At room temperature, the anion **1** is not stable in dichloromethane: ^{1}H NMR spectra show the slow appearance of the "disproportionation" reaction depicted in Equation (3) and in

$$2[Re_3(\mu\text{-H})_4(CO)_9(Hpz)]^- \rightarrow [Re_3(\mu\text{-H})_3(CO)_9(\mu\text{-}\eta^2\text{-pz})(Hpz)]^- + [Re_3(\mu_3\text{-H})(\mu\text{-H})_3(CO)_9]^- + H_2 \quad (3)$$

Scheme 2, which affords the starting anion **2** and the previously reported[9] anion $[Re_3(\mu\text{-H})_3(CO)_9(\mu\text{-}\eta^2\text{-pz})(Hpz)]^-$ (**4**). After 10 hours at room temperature, the amount

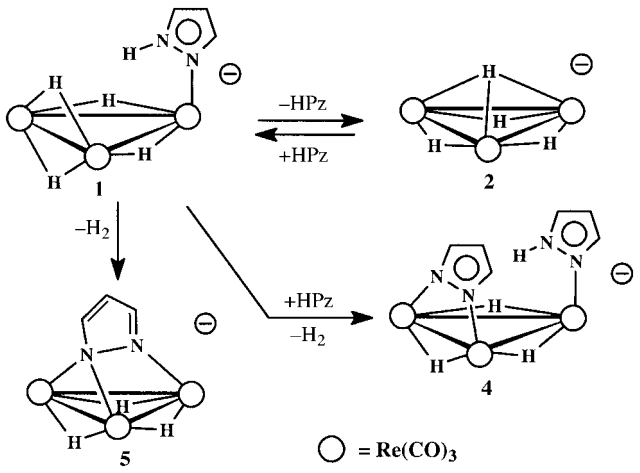

Scheme 2.

of each of the two products corresponded to ≈2.5% and it was roughly doubled after 20 hours.

A two-dimensional NOESY experiment at 300 K shows exchange cross-peaks between the hydridic signals of **1** and those of **2**. This exchange implies lability of the pyrazole ligand in **1**, namely fast reversibility of reaction (1). Such lability provides a reasonable two-step mechanism for the disproportionation process of reaction (3). Indeed, the molecules of free pyrazole, generated by the dissociation of **1**, in addition to re-reacting with **2** according to Equation (1), can also react with **1** (less reactive but present in a much higher concentration) according to the previously reported reaction given in Equation (4),[9] which affords the anion **4**.

$$[Re_3(\mu\text{-H})_4(CO)_9(Hpz)]^- + Hpz \rightarrow [Re_3(\mu\text{-H})_3(CO)_9(\mu\text{-}\eta^2\text{-pz})(Hpz)]^- + H_2 \quad (4)$$

This slow but irreversible reaction consumes pyrazole molecules and causes the progressive increase of the concentration of the anions **2** and **4**, according to the overall Equation (3).

The novel anion $[Re_3(\mu\text{-H})_3(CO)_9(\mu_3\text{-}\eta^2\text{-pz})]^-$ (5): The ^{1}H NMR spectra of CD_2Cl_2 solutions of the anion **1** show the slow formation not only of the anions **2** and **4**, but also of another pyrazole-containing species with a single hydridic resonance at $\delta = -11.71$ (molar fraction ≈0.12 after 20 hours). The formation of such a species is much faster in acetone, in which it becomes the main product after several hours (molar fraction ≈0.7 after 20 hours).[29] The NMR data of the novel species **5** indicate that it contains three hydrides and one "symmetrical" pyrazolato ligand (two signals in the ratio 2:1). It is therefore formulated as the $[Re_3(\mu\text{-H})_3(CO)_9(pz)]^-$ anion, formed according to Equation (5). The evolution of H_2 has been confirmed by the growth of its signal at $\delta = 4.5$.

$$[Re_3(\mu\text{-H})_4(CO)_9(Hpz)]^- \rightarrow [Re_3(\mu\text{-H})_3(CO)_9(pz)]^- + H_2 \quad (5)$$

Further support of this hypothesis has been provided by the synthesis of **5** through a different pathway that involved the reaction of one equivalent of pyrazole with the [Re$_3$-

$(\mu\text{-H})_3(CO)_9(\mu_3\text{-}CH_3)]^-$ anion, which contains a methyl group bridging the three metal atoms of the triangle.[30] In this case, the reaction is also fast in CH_2Cl_2 and affords **5** as the main reaction product in a few hours at room temperature, according to Equation (6). ^{1}H NMR spectra show the

$$[Re_3(\mu\text{-H})_3(CO)_9(\mu_3\text{-}CH_3)]^- + Hpz \rightarrow [Re_3(\mu\text{-H})_3(CO)_9(pz)]^- + CH_4 \quad (6)$$

intermediate formation of two species, tentatively formulated as the *syn* and *anti* isomers of the adduct $[Re_3(\mu\text{-H})_3(CO)_9(\mu\text{-}CH_3)(HPz)]^-$ (**6a**, **6b**) shown in Scheme 3. The faster formation of **5** in reaction (6) with respect to reaction (5) indicates that the bridging methyl group of **6** is more susceptible toward electrophilic attack by the acidic pyrazole proton than the bridging hydrides of **1**.

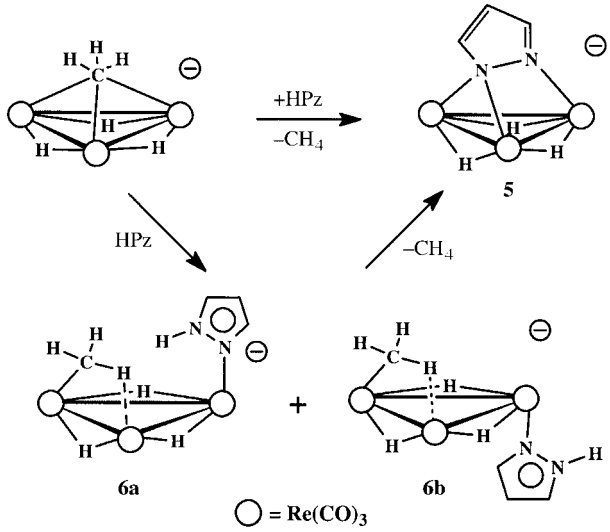

Scheme 3.

X-ray diffraction analysis of crystals of the $[NEt_4]^+$ salt of **5** has confirmed its structure and revealed that the pyrazolate anion bridges all three Re atoms of the triangular cluster, as depicted in Scheme 3 and Figure 7.

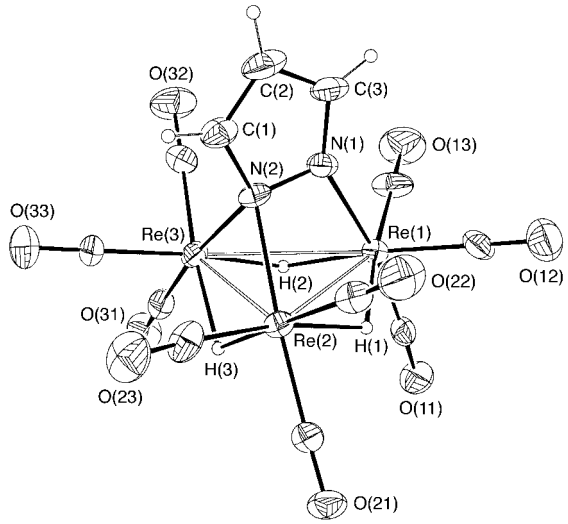

Figure 7. ORTEP drawing of the $[Re_3(\mu\text{-H})_3(CO)_9(\mu_3\text{-}\eta^2\text{-pz})]^-$ anion (**5**) with a partial labelling scheme. Thermal ellipsoids are drawn at the 30% probability level. Hydrogen atoms were given arbitrary radii.

The C_s symmetry revealed by the solid-state structure (see below) would imply two hydridic resonances in a 1:2 ratio. The presence of only one hydridic resonance, even at a very low temperature (193 K),[31] indicates the fast rotation of the pyrazolato ligand on the surface of the triangular cluster, through the interchange of the bridging and terminal coordination modes of the two pyrazole nitrogen atoms.

In the presence of donor ligands, the novel μ_3 coordination of pyrazole is replaced by the more common μ coordination, as shown by the reaction of **5** with pyrazole; this occurs instantaneously and quantitatively at room temperature, according to Equation (7).

$$[Re_3(\mu\text{-H})_3(CO)_9(\mu_3\text{-}\eta^2\text{-pz})]^- + Hpz \rightarrow [Re_3(\mu\text{-H})_3(CO)_9(\mu\text{-}\eta^2\text{-pz})(Hpz)]^- \quad (7)$$

To understand which parameter induces the large change observed in the rate of reaction (5) on passing from CH_2Cl_2 to acetone, we performed the same reaction (under the same conditions of temperature and concentration) in two other solvents, namely $[D_8]$tetrahydrofuran (THF) and $[D_7]$dimethylformamide (DMF). ^{1}H NMR monitoring shows that, in the former solvent, the formation of the anion **5** is about as slow as in CH_2Cl_2. While in $[D_7]$DMF, the disappearance of **1** is very fast and after 10 minutes the ^{1}H NMR spectrum shows essentially only one species, which can be formulated as the triangular cluster anion $[Re_3(\mu\text{-H})_3(CO)_9(\mu\text{-}\eta^2\text{-pz})(DMF)]^-$ (**7**); this anion contains a (deuterated) DMF molecule terminally coordinated to the cluster vertex opposite to the edge bridged by the pyrazolato ligand (see the Experimental Section). The anion **7** can be considered to be a solvent-stabilised form of the anion **5**, formed in reaction (8), analogous to reaction (7). Indeed, the reaction mixture exhibits a very weak hydridic resonance at $\delta = -11.73$, attributable to **5** ($\approx$2.5%, on the base of the integrated intensities) in equilibrium with **7** [Eq. (8)]. Solvent removal (by evaporation to dryness) and dissolution in CD_2Cl_2 affords a solution that exhibits only the resonances of anion **5**. The latter reaction provides the best preparative route to anion **5** (see the Experimental Section).

$$[Re_3(\mu\text{-H})_3(CO)_9(\mu_3\text{-}\eta^2\text{-pz})]^- + DMF \rightleftharpoons [Re_3(\mu\text{-H})_3(CO)_9(\mu\text{-}\eta^2\text{-pz})(DMF)]^- \quad (8)$$

X-ray crystal structure of [NEt4]5: The structure of crystals of the $[NEt_4]^+$ salt of anion **5** consists of discrete anions and cations packed with normal van der Waals contacts. The molecular structure of anion **5** is depicted in Figure 7 (with a partial labelling scheme). A selection of bond parameters is reported in Table 1.

Anion **5** possesses an overall idealised C_s symmetry and contains a metal core of three Re atoms arranged as an isosceles triangle with all edges bridged by one hydrido ligand. Each of the rhenium atoms also bears three terminal carbonyl ligands with facial coordination. With regards to the bonding interactions around the rhenium atoms, each metal attains a distorted octahedral coordination given by three carbonyls, two hydrides and one nitrogen atom, if the direct metal–metal interactions are neglected. With reference to the parent

  0947-6539/02/0823-5346 $ 20.00+.50/0 *Chem. Eur. J.* **2002**, *8*, No. 23

compound **1**, the Re(2)–Re(3) edge, originally bridged by two hydrides, is now spanned by a hydride and the N(2) nitrogen atom of the pyrazole ligand, which is itself bound through N(1) to Re(1) (see Figure 7). An analogous μ_3-η^2 coordination for a pyrazolato ligand has been previously reported for very few lanthanide and alkaline metal complexes.[32] However, anion **5** constitutes the first example in which this coordination mode is obtained on a triangular cluster face made up of transition metal atoms of the *d* block.

The two long hydrogen-bridged Re(1)–Re(2,3) bonds (mean value 3.172 Å) fall into the range usually found for Re(μ-H)Re interactions. The short Re(2)–Re(3) bond length (2.954 Å) is longer than that usually found for formal Re-(μ-H)$_2$Re double bonds[11, 12] and closer to that typical of Re-(μ-H)(μ-X)Re bonds in which a more-than-two-electron donor atom X has replaced a hydride, as in [Re$_3$-(μ-H)$_3$(CO)$_9$(μ_3-η^2-2-amido-6-methylpyridine)]$^-$ (2.927(1) Å),[33] in [Re$_3$(μ-H)$_3$(CO)$_{10}$(μ-2-propanolato)]$^-$ (2.930(1) Å),[34] and in [Re$_3$(μ-H)$_3$(CO)$_{10}$(μ-Cl)]$^-$ (2.995(2) Å).[35]

The donation of more than two electrons by atom N(2) implies a loss of aromaticity of the pyrazolato moiety; in particular, double bonds should be localised between C(1)–C(2) and N(1)–C(3). Indeed, in anion **5** the C(1)–C(2) bond length (1.329 Å) is shortened, while the C(2)–C(3) bond length (1.398 Å) is lengthened, with respect to the values typical[13] for an aromatic μ-η^2-pyrazolato ligand (d(C–C) = 1.364 Å). Similar considerations can be made for the N–C bond lengths: the N(1)–C(3) bond (1.310 Å) is shortened, while N(2)–C(1) (1.354 Å) is lengthened, with respect to the values typical for an aromatic pyrazolato ligand (d(N–C) = 1.340 Å).[36]

The Re–N bond lengths in **5** are normal and show, as expected, an increased value for the bridging N(2) atom (mean value 2.244 Å) with respect to the terminal-bonded N(1) atom (2.171 Å). In both **1** and **5**, the carbonyl ligands are linear with Re-C-O angles between 176.2(4)° and 179.8(6)°. The pyrazole and pyrazolato moieties in anions **1** and **5** are planar within the limits of experimental error, the maximum deviation out of the root-mean-square plane being 0.007 Å.

Conclusion

In the first part of this work we have presented the characterisation and the reactivity of an unconventional intramolecular hydrogen bond in which a hydrido ligand bridging a cluster edge acts as proton acceptor from a NH group. The short bond length obtained from T_1 data in a dichloromethane solution is in good agreement with that estimated in the solid state. This evidence, as well as the nOe and the IR data, indicate that this rather weak interaction ($\approx$3 kcal mol^{-1}) is also maintained in solution, leading to the stabilisation of one rotational conformer of the axial isomer of anion **1**. In contrast, in solvents able to act as proton acceptors, a classical *inter*molecular N–H$\cdots$O hydrogen bond replaces the *intra*molecular dihydrogen bond.

It has been previously suggested that intermolecular M–H$\cdots$H–X attractive interactions between one hydride and one Brønsted acid play an important role in the protonation pathway affording dihydrogen complexes, and/or eventually H_2 evolution.[3, 6, 7] In the case of the anion **1**, the intramolecular dihydrogen bond does not seem to provide a very efficient pathway for the hydrogen transfer process, since H_2 evolution (leading to the formation of **5**) occurs very slowly in CH_2Cl_2. As a matter of fact, it is this sluggishness of such a hydrogen transfer that makes the anion **1** stable enough to be accurately characterised, even at room temperature. By contrast, the much faster proton transfer from pyrazole to the bridging methyl group in anions **6** [Eq. (6)] made the characterisation of these transient intermediates difficult.

In fact the bridging coordination of the proton-acceptor hydride is expected to reduce not only its thermodynamic, but also its kinetic "hydricity" with respect to a terminal hydride, because of the instability of the expected transition state (an until now unknown bridging dihydrogen molecule). The marked increase of the rate in donor solvents, such as acetone or DMF, might support the hypothesis that H_2 evolution occurs through a two-step process in which the solvent acts as a nucleophile by coordinating to the unsaturated anion **1** to give a saturated derivative with a terminal hydrido ligand, which in turn is highly susceptible to protonation by the acidic NH proton. However, the behaviour of **1** in THF (a donor solvent as good as acetone) conflicts with this hypothesis.

Therefore, it is likely that a key role is played by the dielectric constant of the solvent, which is high for acetone and DMF and much lower for THF and CH_2Cl_2. Indeed, a highly polar transition state is expected for rate-determining ionisation of the N–H bond (either intra- or inter-molecular). In the latter hypothesis, the solvent or adventitious water[37] would play the role of a proton carrier from the pyrazole to the hydride.

Whatever the actual mechanism of H_2 evolution, the protonation of the hydride and the hydrogen loss creates a vacant coordination site and prompts the pyrazolate anion to adopt the novel coordination mode in which it acts as a bridging ligand toward three metal centres. This finding confirms the capability of metal clusters to favour polycentric interactions and unusual pathways for the activation of organic substrates.

Experimental Section

General: The reactions were performed under N_2 with Schlenk techniques. Solvents were dried and deoxygenated by standard methods. Pyrazole (Fluka) was used as received. Published methods were used for the syntheses of [NEt$_4$][Re$_3$(μ_3-H)(μ-H)$_3$(CO)$_9$],[38] [Re$_3$(μ-H)$_3$(CO)$_{11}$-(NCMe)][39] and [PPh$_4$][Re$_3$(μ-H)$_3$(CO)$_9$(μ_3-CH$_3$)].[30] The NMR spectra were acquired on Bruker AC200 or DRX300 spectrometers. Infrared spectra were obtained with a Bruker Vector 22FT instrument. Low-temperature IR spectra were acquired on a variable-temperature Graseby Specac cell P/N21525.

Synthesis of [NEt$_4$][Re$_3$(μ-H)$_4$(CO)$_9$(Hpz)] ([NEt$_4$]1): A sample of [NEt$_4$][Re$_3$(μ_3-H)(μ-H)$_3$(CO)$_9$] (33.2 mg, 0.0351 mmol) in THF (4 mL) was treated at room temperature with pyrazole (3 mg, 0.044 mmol), causing a sudden change of colour from sun yellow to green yellow. IR monitoring after 15 minutes showed the completion of the reaction. The solution was evaporated to dryness, the residue dissolved in CH_2Cl_2 and treated with *n*-hexane to give a pale yellow precipitate, which was dried under vacuum

(30.2 mg, 0.0297 mmol. Isolated yield: 85%); IR (CH_2Cl_2): $\tilde{\nu}$(CO) = 2036 (m), 2004 (vs), 1914 cm^{-1} (s); ^1H NMR (CD_2Cl_2, 298 K): δ = 10.24 (s, 1H; NH), 7.76 (1H; H_γ), 7.40 (1H; H_α), 6.26 (1H; H_β), −7.73 (s, 1H; H_a), −9.03 (s, 1H; H_b), −9.68 ppm (s, 2H; H_c); ^1H NMR ([D_6]acetone, 298 K) δ = 11.86 (s, 1H; NH), 7.70 (1H; H_α), 7.68 (1H; H_γ), 6.25 (1H; H_β), −7.62 (s, 1H; H_a), −8.71 (s, 1H; H_b), −9.64 ppm (s, 2H; H_c); ^{13}C NMR (CD_2Cl_2, 295 K): δ = 197.82 (2C; CO), 196.08 (2C; CO), 194.21 (1C; CO), 192.45 (2C; CO), 189.42 (2C; CO), 145.90 (1C; $C_\gamma$pz), 129.95 (1C; $C_\alpha$pz), 107.18 ppm (1C; $C_\beta$pz); elemental analysis calcd (%) for $C_{20}H_{28}N_3O_9Re_3$ (1013.4): C 23.70, H 2.78, N 4.15; found: C 24.04, H 2.75, N 4.45.

[PPh_4][$Re_3(\mu$-H)$_4$(CO)$_9$(Hpz)] ([PPh_4]1): The $[PPh_4]^+$ salt of anion **1** was obtained in the same way as the $[NEt_4]^+$ salt from [PPh_4][$Re_3(\mu$-H)$_3(\mu_3$-H)(CO)$_9$]. Crystals of [PPh_4]**1** that were suitable for X-ray analysis were obtained by slow diffusion of *n*-hexane into a concentrated solution of [PPh_4]**1** in CH_2Cl_2.

Substitution of MeCN by Hpz in [$Re_3(\mu$-H)$_3$(CO)$_{11}$(NCMe)]: A solution of [$Re_3(\mu$-H)$_3$(CO)$_{11}$(NCMe)] (13 mg, 0.013 mmol) in CH_2Cl_2 (2 mL) was treated with pyrazole (10.5 mg, 0.154 mmol) and stirred overnight at room temperature. The colourless solution was evaporated to dryness, and the residue was washed with water to remove the excess pyrazole and crystallised from CH_2Cl_2/*n*-hexane, affording 8.7 mg (0.008 mmol) of spectroscopically pure **3**. IR (CH_2Cl_2, 298 K): $\tilde{\nu}$(CO) = 2115 (w), 2092 (m), 2032 (vs), 2018 (s), 2005 (s), 1967 (m), 1933 (m), 1919 cm^{-1} (mw); ^1H NMR (CD_2Cl_2, 298 K): δ = 10.12 (s, 1H; NH), 7.76 (1H; $H_{\alpha,\gamma}$), 7.61 (1H; $H_{\gamma,\alpha}$), 6.39 (1H; H_β), −13.58 (s, 2H), −17.20 ppm (s, 1H).

Variable-temperature T_1 and nOe measurements on 1 in CD_2Cl_2 and [D_6]acetone: A solution of [PPh_4]**1** (15.0 mg, 0.0123 mmol) in CD_2Cl_2 (0.5 mL) in an NMR tube was degassed through repeated freeze–thaw cycles. ^1H NMR variable-temperature spectra were acquired on a Bruker AC200 spectrometer at 183–298 K. In the same range of temperatures, ^1H T_1 values were obtained by the three-parameter fit of the intensities of the signals in the spectra recorded with the standard nonselective inversion recovery pulse sequence with 12 variable delays. The results are reported in Tables 3 and 4 and the estimated accuracy is better than 5%. The same sample was also used for nOe experiments performed at 223 K. Saturation radio-frequency fields were applied for 100 ms on and off resonance with respect to the selected signal. The acquisitions were cycled until a good signal-to-noise was achieved in the spectra obtained through the Fourier transform of the difference on the free induction decays (FIDs). Irradiation of the NH signal resulted in a significant enhancement of the signal of H_b and in a much smaller one of the signal of H_c. A corresponding enhancement of the intensity of NH proton resonance was observed when both the latter signals were irradiated. The variable-temperature ^1H chemical shift and T_1 values in [D_6]acetone from 183 K to 298 K were obtained at 7.1 T, on a sample of [NEt_4]**1** (11.8 mg, 0.0116 mmol) dissolved in the solvent (0.5 mL; Tables 3 and 5). For T_1 measurements 16 variable delays were employed and the results analysed as described above.

Two-dimensional NOESY experiments on [NEt_4]1 in different solvents: The ^1H two-dimensional NOESY phase-sensitive experiment shown in Figure 4 was performed on a solution of [NEt_4]**1** (17.5 mg, 0.0172 mmol) in CD_2Cl_2 (0.5 mL) at 300 K (4.7 T, τ_m = 1 s, 32 FIDs, sweep width (SW) = 4587 Hz, 1 K data points for 420 experiments). Shifted sine-bell functions were applied in both dimensions before the Fourier transform and after zero-filling to 1 K in *F*1. Other ^1H two-dimensional NOESY phase-sensitive experiments at 300 K in CD_2Cl_2 were performed at 7.1 T (22.2 mg, 0.0219 mmol, τ_m = 3 s, 16 FIDs, SW = 10482 Hz, 1 K data points for 512 experiments) and transformed as above. The experiment shown in Figure 6 was performed at 298 K at 7.1 T on a sample of [NEt_4]**1** (11.8 mg, 0.0116 mmol) dissolved in [D_6]acetone (0.5 mL) with τ_m of 2.0 s (16 FIDs, SW = 10482 Hz, 1 K data points 512 experiments) and transformed as above.

Reaction of [PPh_4][$Re_3(\mu$-H)$_3$(CO)$_9(\mu_3$-CH_3)] with Hpz: A solution of [PPh_4][$Re_3(\mu$-H)$_3$(CO)$_9(\mu_3$-CH_3)] (7.0 mg, 0.0060 mmol) in CH_2Cl_2 (2 mL) was treated with pyrazole (86 μL of a solution 0.067 M in CH_2Cl_2, 0.0058 mmol). The mixture was stirred at room temperature for about 15 minutes and then evaporated to dryness. The residue was dissolved in CD_2Cl_2 (0.5 mL) and the progress of the reaction was monitored by ^1H NMR spectroscopy at 300 K. After 20 minutes, and in addition to the signals of the starting material (12.3% of the mixture), the spectrum showed the following hydridic resonances: δ = −2.79 (s, 3H; CH_3), −10.82 (s, 1H), −12.67 ppm (s, 2H) and δ = −3.91 (s, 3H; CH_3), −9.89 (s, 1H), −12.20 ppm (s, 2H), attributable to the two isomers of adduct **6** (4.1% and 12.3%, respectively); δ = −11.71 ppm (3H) assigned to anion **5** (46.6%); δ = −9.80 (s, 2H), −11.18 (s, 1H), and δ = −10.70 (s, 2H), −11.78 ppm (s, 1H) attributable to the *syn* and *anti* isomers of the anion [Re_3-(μ-H)$_3$(CO)$_9$(μ-η^2-pz)(Hpz)]$^-$ (**4**) (overall amount 24.6%). After 2.5 h, the spectrum indicated the following composition of the mixture: starting material 4.7%; **5** 74%; **4** 20.5%. Addition of further 100 μL of the pyrazole solution completed the conversion of both the starting material and the anion **5** into the anion **4**.

^1H NMR monitoring of the behaviour of [NEt_4]1 in different solvents at room temperature: A sample of [NEt_4]**1** (6.8 mg, 0.0067 mmol) was dissolved at room temperature in [D_6]acetone, directly in an NMR tube. The solution was kept at 273 K until it was introduced into the NMR probe thermostated at 300 K. Automatic acquisition of the spectra every hour was performed for 20 hours. Other spectra were acquired at irregular intervals for three further days. The same procedure was followed for the experiments in CD_2Cl_2 and in [D_8]THF, with isolated crystals of [NEt_4]**1** (≈7 mg). Isolated crystals (5.6 mg) were also used for the experiment in [D_7]DMF. In this case, however, the disappearance of **1** was very fast and after 10 minutes the spectrum showed only two hydridic signals: at δ = −8.43 (2H) and −11.16 ppm (1H), attributed to [$Re_3(\mu$-H)$_3$(CO)$_9$(μ-η^2-pz)(DMF)]$^-$, whose pyrazole signals were at δ = 7.15 (2H), 5.85 ppm (1H). The sample was evaporated to dryness and the residue was dissolved in CD_2Cl_2 at room temperature. The ^1H NMR spectrum of this solution showed the presence of the anion **5** only.

Synthesis of [PPh_4]5: A sample of [PPh_4]**1** (23 mg, 0.0188 mmol) was dissolved in DMF (1 mL). The colour of the solution rapidly faded and IR monitoring after 20 minutes showed a novel set of ν(CO) bands, attributable to the anion **7** (2029 (m), 1999 (vs), 1905 (br, vs), 1870 cm^{-1} (sh)). The solution was evaporated to dryness and the residue dissolved in CH_2Cl_2. Addition of *n*-hexane gave an oily precipitate that became solid after vigorous stirring for 2 h. The cream precipitate was crystallised from CH_2Cl_2/*n*-hexane, affording analytically pure [PPh_4]**5** (16.1 mg, 0.0132 mmol, isolated yields 70.2%). Elemental analysis calcd (%) for $C_{36}H_{26}N_2O_9PRe_3$ (1220.5): C 35.43, H 2.15, N 2.30; found: C 35.39, H 1.95, N 2.07; IR (CH_2Cl_2): $\tilde{\nu}$(CO) = 2008 (vs), 1916 cm^{-1} (br, vs); ^1H NMR (CD_2Cl_2, 298 K): δ = 7.37 (2H; $H_{\alpha,\gamma}$), 6.16 (1H; H_β), −11.81 ppm (s, 3H). The same procedure was used for the synthesis of [NEt_4]**5**. Crystals of the latter salt suitable for single crystal X-ray analysis were grown from CH_2Cl_2/*n*-hexane at 248 K.

X-ray structural analysis:

Collection and reduction of X-ray diffraction data: Suitable crystals were mounted on a glass fibre tip and affixed to a goniometer head. Single-crystal X-ray diffraction data were collected on a Siemens SMART CCD area detector diffractometer, with graphite-monochromated $Mo_{K\alpha}$ radiation (λ = 0.71073 Å) at room temperature (295(2) K) for [NEt_4]**5** and at 173(2) K for [PPh_4]**1**. Unit cell parameters were initially obtained from ≈100 reflections ($5 < \theta < 25^\circ$) taken from 45 frames collected in three different ω regions, and eventually refined against a large number of reflections (≈8000). For [PPh_4]**1**, a full sphere of reciprocal space was scanned by 0.3° ω steps, collecting 2500 frames each at 15 s exposure and keeping the detector at 5.50(2) cm from the sample. For [NEt_4]**5**, a full sphere of reciprocal space was scanned by 0.3° ω steps, collecting 2000 frames each at 60 s exposure and keeping the detector at 3.00(2) cm from the sample. Intensity decay was monitored by recollecting the initial 100 frames at the end of data collection and analysing the duplicate reflections. The collected frames were processed for integration (SAINT[40]); an empirical absorption correction was made on the basis of the symmetry-equivalent reflection intensities collected (SADABS[41]). Crystal data and data collection parameters are summarised in Table 6.

Structure solution and refinement: The structures were solved by direct methods (SIR 97[42]) and subsequent Fourier synthesis; they were refined by full-matrix least-squares on F^2 (SHELX 97[43]) by using all reflections. Scattering factors for neutral atoms and anomalous dispersion corrections were taken from the internal library of SHELX 97. Weights were assigned to individual observations according to the formula $w = 1/[\sigma^2(F_o^2) + (aP)^2]$, where $P = (F_o^2 + 2F_c^2)/3$; the parameter *a* was chosen to give a flat analysis of variance in terms of F_o^2. Anisotropic displacement parameters were assigned to all non-hydrogen atoms. To correctly assign atoms N(2) and

0947-6539/02/0823-5348 $ 20.00+.50/0 *Chem. Eur. J.* **2002**, *8*, No. 23

Table 6. Crystallographic data for the trinuclear complexes $[PPh_4]$**1** and $[NEt_4]$**5**.

	$[PPh_4]$**1**	$[NEt_4]$**5**
formula	$C_{36}H_{28}N_2O_9PRe_3$	$C_{20}H_{26}N_3O_9Re_3$
M_r	1222.17	1011.04
crystal system	triclinic	tetragonal
space group	$P\bar{1}$ (No. 2)	$P\bar{4}2_1c$ (No. 114)
a[Å]	11.189(6)	18.830(6)
b[Å]	13.207(7)	
c[Å]	14.691(8)	15.930(8)
α[°]	64.280(10)	
β[°]	73.360(10)	
γ[°]	89.420(10)	
V[Å^3]	1857.5(17)	5648(4)
T[K]	173(2)	295(2)
Z	2	8
$F(000)$	1140	3712
ρ_{calcd}[g cm^{-1}]	2.185	2.378
$\mu(Mo_{K\alpha})$[mm^{-1}]	9.849	12.874
crystal habit	yellow prism	orange cube
crystal size[mm]	0.20 × 0.10 × 0.08	0.10 × 0.10 × 0.08
2θ range[°]	4.8–46.6	3.0–46.6
index ranges	$-12 \le h \le 12$	$-20 \le h \le 20$
	$-14 \le k \le 14$	$-20 \le k \le 20$
	$-16 \le l \le 16$	$-17 \le l \le 17$
intensity decay[%]	3	8
min/max transmission	0.307/0.455	0.242/0.357
measured reflections	14887	41859
independent reflections	5318	4058
R_{int},[a]/R_σ[b]	0.0246/0.0311	0.0661/0.0296
observed reflections [$I > 2\sigma(I)$]	4633	3786
data/parameters	5318/461	4058/319
$R(F)$[c] [$I > 2\sigma(I)$]	0.0188	0.0321
$wR(F^2)$[d] (all data)	0.0397	0.0559
goodness-of-fit S[e]	0.957	1.291
$\Delta\rho$max/min [e Å^{-3}]	0.571/−0.967	0.841/−0.765

[a] $R_{int} = \Sigma|F_o^2 - F_{mean}^2|/\Sigma|F_o^2|$. [b] $R_\sigma = \Sigma|\sigma(F_o^2)|/\Sigma|F_o^2|$. [c] $R(F) = \Sigma||F_o| - |F_c||/\Sigma|F_o|$. [d] $wR(F^2) = [\Sigma w(F_o^2 - F_c^2)^2/\Sigma wF_o^4]^{1/2}$. [e] $S(F^2) = [\Sigma w(F_o^2 - F_c^2)^2/(n-p)]^{1/2}$ where n is the number of reflections and p is the number of refined parameters.

C(3) in $[PPh_4]$**1**, a refinement was made in which a mixed occupation of the number two site by nitrogen and carbon was allowed. The refinement resulted in an occupation of the site labelled N(2) and C(3) by 100% nitrogen and 100% carbon, respectively. An attempt to refine a model with the opposite occupation resulted in an unrealistically large (small) thermal factor for the hypothetical nitrogen (carbon) atom. Moreover, the assignment is fully consistent with the expected values for N(1)−N(2) and N(1)−C(3) bond lengths. Hydrido ligands were initially evidenced by a difference Fourier map; their positions were in agreement with the local stereogeometry around the metal centres. They were eventually constrained in more accurate positions (calculated with the program HYDEX,[44] with $d(Re{-}H) = 1.85$ Å) with a common refined isotropic displacement parameter. Hydrogen atoms of the tetraphenylphosphonium and tetraethylammonium cations, as well as those of the pyrazole and pyrazolato ligands, were placed in idealised positions and refined riding on their parent atom with an isotropic displacement parameter 1.2 times that of the pertinent carbon or nitrogen atom. The crystal of $[NEt_4]$**5** was a racemic twin, and the ratio of the twin components refined to 0.579(18):0.421(18).[45] The final difference electron-density maps showed no features of chemical significance, with the largest peaks lying close to the metal atoms. Final conventional agreement indexes and other structure refinement parameters are listed in Table 6.

CCDC-184549 ($[PPh_4]$**1**) and CCDC-184548 ($[NEt_4]$**5**) contain the supplementary crystallographic data for this paper. These data can be obtained free of charge via www.ccdc.cam.ac.uk/conts/retrieving.html (or from the Cambridge Crystallographic Data Centre, 12 Union Road, Cambridge CB2 1EZ, UK; fax: (+44) 1223-336033; or deposit@ccdc.cam.uk).

Acknowledgements

Financial support from CNR (CSMTBO) and from Italian MURST (COFIN 2000, Project "Metal Cluster, Basic and Functional Aspect" and FIRB, Project "Intra- and Intermolecular Weak Interactions") is greatly acknowledged.

[1] G. A. Jeffrey, *An Introduction to Hydrogen Bonding*, Oxford University Press, New York, **1997**.
[2] a) M. J. Calhorda, *Chem. Commun.* **2000**, 801–809; b) L. Alkorta, I. Rozas, J. Elguero, *Chem. Soc. Rev.* **1998**, *27*, 163–170; c) R. H. Crabtree, O. Eisenstein, G. Sini, E. Peris, *J. Organomet. Chem.* **1998**, *567*, 7–11; d) E. S. Shubina, N. V. Belkova, L. M. Epstein, *J. Organomet. Chem.* **1997**, *536*, 17–29.
[3] a) R. Custelcean, J. E. Jackson, *Chem. Rev.* **2001**, *101*, 1963–1980; b) R. H. Crabtree, *Science* **1998**, *282*, 2000–2001; c) R. H. Crabtree, P. E. M. Siegbahn, O. Eisenstein, A. L. Rheingold, T. F. Koetzle, *Acc. Chem. Res.* **1996**, *29*, 348–354.
[4] R. H. Crabtree *J. Am. Chem. Soc.* **1995**, *117*, 12875–12876.
[5] a) J. C. Lee, A. L. Rheingold, B. Muler, P. S. Pregosin, R. H. Crabtree, *J. Chem. Soc. Chem. Commun.* **1994**, 1021–1022; b) A. J. Lough, S. Park, R. Ramachandran, R. H. Morris, *J. Am. Chem. Soc.* **1994**, *116*, 8356–8357; c) S. Park, R. Ramachandran, A. J. Lough, R. H. Morris, *J. Chem. Soc. Chem. Commun.* **1994**, 2201–2202; d) E. Peris, J. C. Lee, R. H. Crabtree, *J. Chem. Soc. Chem. Commun.* **1994**, 2573 ; d) J. C. Lee, E. Peris, A. L. Rheingold, R. H. Crabtree, *J. Am. Chem. Soc.* **1994**, *116*, 11014–11019.
[6] a) E. S. Shubina, N. V. Belkova, A. N. Krylov, E. V. Vorontsov, L. M. Epstein, D. G. Gusev, N. Niedermann, H. Berke, *J. Am. Chem. Soc.* **1996**, *118*, 1105–1112; b) A. Messmer, H. Jacobsen, H. Berke, *Chem. Eur. J.* **1999**, *5*, 3341–3349.
[7] a) M. V. Baker, L. D. Field, D. J. Young, *J. Chem. Soc. Chem. Commun.* **1988**, 546–548; b) S. Feracin, T. Bürgi, V. I. Bakhmutov, I. Eremenko, E. V. Vorontsov, A. B. Vimenits, H. Berke, *Organometallics* **1994**, *13*, 4194–4202; c) P. A. Maltby, M. Schlaf, M. Steinbeck, A. J. Lough, R. H. Morris, W. T. Klooster, T. F. Koetzle, R. C. Srivastava, *J. Am. Chem. Soc.* **1996**, *118*, 5396–5407; d) R. H. Morris, *Can. J. Chem.* **1996**, *74*, 1907–1915; e) J. A. Ayllón, C. Gervaux, S. Sabo-Etienne, B. Chaudret, *Organometallics* **1997**, *16*, 2000–2002; f) G. Orlova, S. Scheiner, *J. Phys. Chem. A* **1998**, *102*, 260–269; g) G. Orlova, S. Scheiner, *J. Phys. Chem. A* **1998**, *102*, 4813–4818; h) E. S. Shubina, N. V. Belkova, E. V. Bakhmutova, E. V. Vorontsov, V. I. Bakhmutov, A. V. Ionidis, C. Bianchini, L. Marvelli, M. Peruzzini, L. M. Epstein, *Inorg. Chim. Acta* **1998**, *280*, 302–307; i) M. G. Basallote, J. Durán, M. J. Fernández-Trujillo, M. A. Máñez, J. Rodríguez de la Torre, *J. Chem. Soc. Dalton Trans.* **1998**, 745–750; j) S. Gründemann, S. Ulrich, H.-H. Limbach, N. S. Golubev, G. S. Denisov, L. M. Epstein, S. Sabo-Etienne, B. Chaudret, *Inorg. Chem.* **1999**, *38*, 2550–2551; k) V. I. Bakhmutov, C. Bianchini, M. Peruzzini, F. Vizza, E. V. Vorontsof, *Inorg. Chem.* **2000**, *39*, 1655–1660; l) M. G. Basallote, J. Durán, M. J. Fernández-Trujillo, M. A. Máñez, *J. Organomet. Chem.* **2000**, *609*, 29–35; m) N. V. Belkova, E. S. Shubina, E. I. Gutsul, L. M. Epstein, I. L. Eremenko, S. E. Nefedov, *J. Organomet. Chem.* **2000**, *610*, 58–70.
[8] a) S. Aime, R. Gobetto, E. Valls, *Organometallics* **1997**, *16*, 5140–5141; b) S. Aime, M. Ferriz, R. Gobetto, E. Valls, *Organometallics* **1999**, *18*, 2030–2032; c) S. Aime, M. Ferriz, R. Gobetto, E. Valls, *Organometallics* **2000**, *19*, 707–710; d) S. Aime, E. Diana, R. Gobetto, M. Milanesio, E. Valls, D. Viterbo *Organometallics* **2002**, *21*, 50–57.
[9] T. Beringhelli, G. D'Alfonso, M. Panigati, F. Porta, P. Mercandelli, M. Moret, A. Sironi, *Organometallics* **1998**, *17*, 3282–3292.
[10] a) T. Beringhelli, G. D'Alfonso, *J. Chem. Soc. Chem. Commun.* **1994**, 2631–2632; b) H. C. Horng, C. P. Cheng, C. S. Yang, G.-H. Lee, *Organometallics* **1996**, *15*, 2543–2547.
[11] a) T. Beringhelli, G. Ciani, G. D'Alfonso, H. Molinari, A. Sironi, *Inorg. Chem.* **1985**, *24*, 2666–2671; b) G. Ciani, G. D'Alfonso, M. Freni, P. Romiti, A. Sironi, A. Albinati, *J. Organomet. Chem.* **1977**, *136*, C49–C51.
[12] T. Beringhelli, G. D'Alfonso, M. Freni, G. Ciani, A. Sironi, *J. Chem. Soc. Dalton Trans.* **1986**, 2691–2697.

[13] CSD version 5.22 (October 2001); F. H. Allen, J. E. Davies, J. J. Galloy, O. Johnson, O. Kennard, C. F. Macrae, E. M. Mitchell, G. F. Mitchell, J. M. Smith, D. G. Watson, *J. Chem. Inf. Comput. Sci.* **1991**, *31*, 187–204.

[14] CSD refcodes PESXUG, RIFKEW, and LEHXAX: a) A. M. Baranger, F. J. Hollander, R. G. Bergman, *J. Am. Chem. Soc.* **1993**, *115*, 7890–7891; b) J. A. Cabeza, I. del Río, V. Riera, F. Grepioni, *Organometallics* **1997**, *16*, 812–815; c) J. A. Cabeza, I. del Río, J. M. Fernández-Colinas, A. Llamazares, V. Riera, *J. Organomet. Chem.* **1995**, *494*, 169–177.

[15] The $d(\mathrm{H}\cdots\mathrm{H})$ values have been computed with the bridging hydride positions reported in the original papers and with N–H bond lengths normalised to 1.0 Å.

[16] The hydrido ligand was placed in a potential energy-optimised position with the program HYDEX.[44] The N–H bond length was fixed to the value found in pyrazole by neutron diffraction (1.024 Å): F. K. Larsen, M. S. Lehmann, I. Søtofte, S. E. Rasmussen, *Acta Chem. Scand.* **1970**, *24*, 3248–3258.

[17] The comparison with the ν(NH) band of free pyrazole would not be meaningful, since pyrazole molecules in the solid state are involved in extensive intermolecular hydrogen-bonding interactions, leading to a broad band at $\nu \approx 3160\ \mathrm{cm}^{-1}$.

[18] A. V. Iogansen, *Hydrogen Bond*, Nauka, Moscow, **1981**, cited in N. V. Belkova, E. S. Shubina, A. V. Ionidis, L. M. Epstein, H. Jacobsen, A. Messmer, H. Berke, *Inorg. Chem.* **1997**, *36*, 1522–1525.

[19] This value compares well with literature data for dilute solutions of pure pyrazole in CCl_4 ($\nu = 3485 \pm 10\ \mathrm{cm}^{-1}$, $\Delta\nu_{1/2} = 20\ \mathrm{cm}^{-1}$).[20] In addition to this sharp band, which is attributable to free pyrazole, pyrazole solutions also show a second, very broad band (at 3400 to 2000 cm^{-1}), whose intensity increases with the concentration. It is attributed to the formation of oligomers through intermolecular hydrogen-bond interactions.[20]

[20] D. M. W. Anderson, J. L. Duncan, F. J. C. Rossotti, *J. Chem. Soc.* **1961**, 140–145.

[21] The slight shift to lower wavenumbers and the broadening of the ν(NH) band of **3** with respect to free pyrazole are probably caused by the increased acidity of the NH proton upon coordination; this causes stronger N–H$\cdots$Cl interactions (with the solvent) in **3** than in free pyrazole.

[22] a) P. Mauret, J. P. Fayet, M. Fabre, *Bull. Soc. Chim. Fr.* **1975**, 1675–1678; b) A. N. Nesmeyanov, E. B. Zavelovich, V. N. Babin, N. S. Kochetkova, E. I. Fedin, *Tetrahedron* **1975**, *31*, 1461–1462.

[23] For solid-state studies concerning chains or cyclic oligomers of pyrazoles see C. Foces-Foces, A. Echevarría, N. Jagerovic, I. Akorta, J. Elguero, U. Langer, O. Klein, M. Minguet-Bonvehí, H.-H. Limbach, *J. Am. Chem. Soc.* **2001**, *123*, 7898–7906, and references therein.

[24] In a two-spin system, the homonuclear intramolecular dipolar relaxation rate is given by Equation (9), where γ_H is the magnetogyric ratio of the hydrogen nucleus, I is the nuclear spin, ω_0 is the Larmor frequency, τ_c is the correlation time, $r_{H\text{–}H}$ is the distance between the two hydrogen atoms and the other symbols have the usual meanings. Therefore, if an estimate of this rate and the correlation time τ_c are known, the distance between the two spins $r_{H\text{–}H}$ can be calculated according to:

$$R_{H\text{–}H} = (T_1)_{H\text{–}H}^{-1} = \frac{\mu_0^2 \gamma_H^4 \hbar^2 I(I+1)}{40\pi^2 r_{H\text{–}H}^6} \tau_c \left[\frac{1}{1+\omega_0^2\tau_c^2} + \frac{4}{1+4\omega_0^2\tau_c^2} \right] \quad (9)$$

Such an equation also predicts that the maximum dipolar relaxation rate (that is the minimum T_1) occurs when $\omega_0\tau_c = 0.616$, and therefore the correlation time at the temperature when the minimum T_1 is known.

[25] The ratio of the cross-peak volumes (NH,H_b) versus (H_γ,H_b) is $\approx$30, while that for (NH,H_c) versus (H_γ,H_c) is $\approx$5.

[26] Note also the interchange of the chemical shifts of H_α ($\delta = 7.70$ vs 7.40 ppm) and H_γ ($\delta = 7.68$ vs 7.76 ppm) in [D_6]acetone with respect to CD_2Cl_2.

[27] The acetone solutions of free pyrazole also showed the resonances of 2-(1-pyrazolyl)propan-2-ol arising from the reversible addition of pyrazole to the carbonyl group of the solvent. a) M. T. Chenon, C. Coupry, D. M. Grant, R. J. Pugmire, *J. Org. Chem.* **1977**, *42*, 659–661; b) A. N. Nesmeyanov, E. B. Zavelovich, V. N. Babin, N. S. Kochetkova, E. I. Fedin, *Tetrahedron* **1975**, *31*, 1463–1464.

[28] The same feature was also observed for the saturated species **3**: in the presence of a small amount of THF in the CD_2Cl_2 solution, the position of the NH signal of **3** showed a significant temperature dependence (from $\delta = 12.32$ ppm at 193 K to $\delta = 10.7$ ppm at 273 K).

[29] In contrast, the molar fractions of the two "disproportionation" products, namely the anions $[Re_3(\mu_3\text{-}H)(\mu\text{-}H)_3(CO)_9]^-$ and $[Re_3(\mu\text{-}H)_3(CO)_9(\mu\text{-}\eta^2\text{-}pz)(Hpz)]^-$, remained very low, as in dicloromethane.

[30] T. Beringhelli, G. D'Alfonso, P. Mercandelli, M. Moret, M. Panigati, F. Porta, A. Sironi, *J. Am. Chem. Soc.* **1999**, *121*, 2307–2308.

[31] On varying the temperature from 193 to 300 K, we only observed a shift of δ (from -12.01 to -11.71) without a significant change of the bandwidth.

[32] CSD refcodes MAPQUP, MAPRAW, MAPREA, PAZXET, VAVZIB and VAVZOH: a) G. B. Deacon, E. E. Delbridge, C. M. Forsyth, B. W. Skelton, A. H. White, *J. Chem. Soc. Dalton Trans.* **2000**, 745–751; b) C. Yélamos, M. J. Heeg, C. H. Winter, *Inorg. Chem.* **1998**, *37*, 3892–3894; c) H. Schumann, P. R. Lee, J. Loebel, *Angew. Chem.* **1989**, *101*, 1073–1074; *Angew. Chem. Int. Ed. Engl.* **1989**, *28*, 1033–1035.

[33] J. A. Cabeza, A. Llamazares, V. Riera, R. Trivedi, F. Grepioni, *Organometallics* **1998**, *17*, 5580–5585.

[34] T. Beringhelli, G. D'Alfonso, M. Freni, G. Ciani, M. Moret, A. Sironi, *J. Organomet. Chem.* **1988**, *339*, 323–332.

[35] G. Ciani, G. D'Alfonso, M. Freni, P. Romiti, A. Sironi, *J. Organomet. Chem.* **1982**, *226*, C31-C35.

[36] Some of these differences are not statistically significant since standard uncertainties of C–C and C–N bond lengths are as large as 0.01 Å. However, the observed trend is consistent with the expected localisation of the double bonds in the pyrazolato moiety.

[37] An experiment performed with carefully anhydrified CD_2Cl_2 showed that the rate of formation of **5** in this solvent was significantly reduced ($\approx$7% of **5** after 29 h).

[38] T. Beringhelli, G. D'Alfonso, M. G. Garavaglia, *J. Chem. Soc. Dalton Trans.* **1996**, 1771–1773.

[39] M. I. Bruce, P. J. Low, *J. Organomet. Chem.* **1996**, *519*, 221–222.

[40] SAINT, Integration Software for Single Crystal Data Frames, Bruker AXS, Madison, WI (USA), **1999**.

[41] G. M. Sheldrick, SADABS, Program for Empirical Absorption Correction, Universität Göttingen, Göttingen (Germany), **1996**.

[42] A. Altomare, M. C. Burla, M. Camalli, G. L. Cascarano, C. Giacovazzo, A. Guagliardi, A. G. G. Moliterni, G. Polidori, R. Spagna, *J. Appl. Crystallogr.* **1999**, *32*, 115–119.

[43] G. M. Sheldrick, SHELX-97, Program for Crystal Structure Refinement, Universität Göttingen, Göttingen (Germany), **1997**.

[44] A. G. Orpen, *J. Chem. Soc. Dalton Trans.* **1980**, 2509–2516.

[45] H. D. Flack, *Acta Crystallogr. Sect. A* **1983**, *39*, 876–881.

Received: May 6, 2002 [F4067]

  0947-6539/02/0823-5350 $ 20.00+.50/0